Comparison of Trend Detection Algorithms in the Analysis of Physiological Time-Series Data

William W. Melek*, *Member, IEEE*, Ziren Lu, Alex Kapps, and William D. Fraser

***Abstract*—This paper presents a comparative performance analysis of various trend detection methods developed using fuzzy logic, statistical, regression, and wavelet techniques. The main contribution of this paper is the introduction of a new method that uses noise rejection fuzzy clustering to enhance the performance of trend detection methodologies. Furthermore, another contribution of this work is a comparative investigation that produced systematic guidelines for the selection of a proper trend detection method for different application requirements. Examples of representative physiological variables considered in this paper to examine the trend detection algorithms are: 1) blood pressure signals (diastolic and systolic); and 2) heartbeat rate based on RR intervals of electrocardiography signal. Furthermore, synthetic physiological data intentionally contaminated with various types of real-life noise has been generated and used to test the performance of trend detection methods and develop noise-insensitive trend-detection algorithms.**

***Index Terms*—Convex fuzzy subsets, first-level wave decomposition, fuzzy scatter matrix, means absolute deviation, trend detection, Trigg's tracking.**

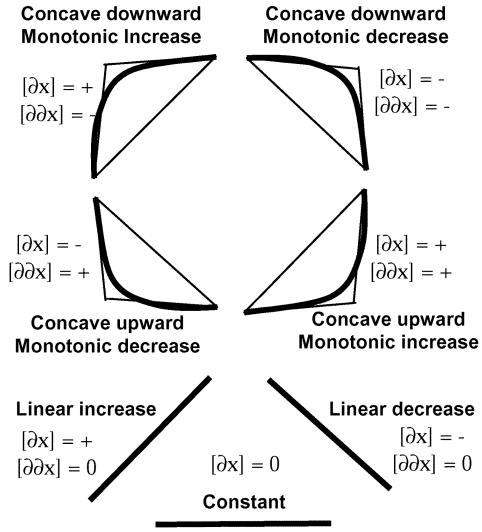

Fig. 1. Labeling of different phases in signal pattern.

I. Introduction

TREND detection has been a practically important way of monitoring a subject's physiological status in intensive care units and operating rooms. The methodologies introduced in this paper has resulted from work on military applications of on-line trend analysis, such as monitoring of wounded soldiers by first-response medical staff at the battlefield and high-acceleration protection of fighter jet pilots. Efficient trend detection methods can provide early warnings, severity assessments of a subject's physiological state, and decision support for first-response medical attendants. Trend analysis involves examining time-series data and identifying significant increases or decreases in the magnitude of a reference variable. Although this can be considered a simple task for a human, to distinguish natural fluctuations from symptomatic tendencies in real-time or close to real-time can be quite intricate for a computerized algorithm. Humans are able to quickly grasp the relevant dynamic pattern from a whole image of a signal and perform filtering and analysis of the data with inexact concepts instead of detailed mathematical computations. In general, many definitions of the term "trend" are in use. In the biomedical field, a trend is seen as a general direction of the mean level in a set of data [3]. Blom *et al.* [4] defined a trend as a slow, consistent, unidirectional change in the value of a variable. Challis *et al.* [5] defined a trend as a steadily rising or steadily falling pattern. Haimowitz *et al.* [6] defined a trend as a clinically significant pattern in a sequence of time-ordered data. Some of the definitions regard a trend as a feature that can be extracted from the course of a variable, while others suggest that a trend is defined as some sort of pattern that occurs in a signal.

Preprocessing time series physiological data will precede the implementation of the trend detection methods presented in this paper. Major components of this preprocessing process are 1) feature attribute derivation and 2) data partitioning [1]. Feature attribute derivation refers to the selection and calculation of mathematical quantities that can describe the time-series data for the task in question. The quantities are calculated over a specific time interval for successive overlapping data. The same quantities can be calculated over multiple time intervals, and then used as two different attributes of that monitored signal. The various quantities calculated for each signal, for all monitored signals of interest, together comprise the set of feature attributes that describe a time period of monitoring. Feature attributes usually consist of multiple parts, corresponding to characteristics of sequential blocks of a monitored signal. For example, a two-phase pattern of data may describe the slope of the first phase and the slope of the second phase of two contiguous regions. These multiphase patterns can be described either by a single attribute that encapsulates the idea of the whole pattern, or by multiple attributes that together paint the picture

Manuscript received April 12, 2004; revised September 26, 2004. *Asterisk indicates corresponding author.*

*W. W. Melek is with the Department of Mechanical Engineering, University of Waterloo, ON N2L 3G1, Canada (e-mail: wael.melek@utoronto.ca).

Z. Lu and A. Kapps are with Engineering Services Inc. (ESI), Toronto, ON M5R 2J7, Canada (e-mail: lu@esit.com; kapps@esit.com).

W. D. Fraser is with the Defence R&D Canada-Toronto, Toronto, ON M3M 3B9, Canada (e-mail: Bill.Fraser@drdc-rddc.gc.ca).

Digital Object Identifier 10.1109/TBME.2005.844029

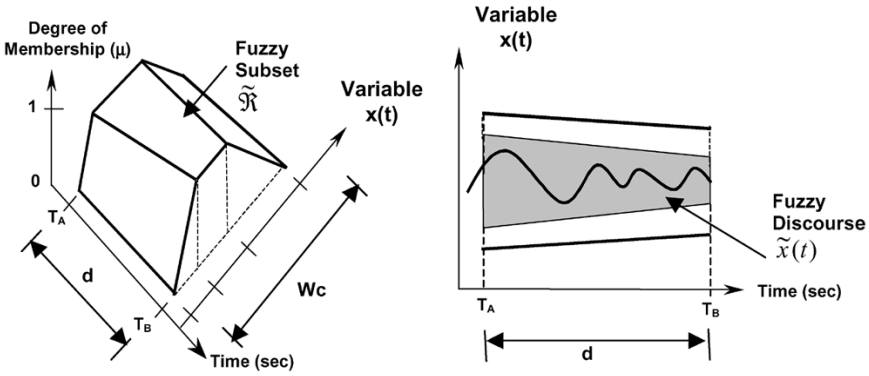

Fig. 2. Representation of a fuzzy trend and compatibility of a signal with a fuzzy trend [2].

of the whole pattern. For instance, if we wish to learn temporal patterns, or trends, consisting of two phases, we consider the case in which each phase is n seconds in length and can be described by only one of three slopes characteristics: positive (rising), zero (level), or negative (falling). There would then be nine unique two-phase patterns. In case of a single-phase, one would end up with one of seven patterns as shown in Fig. 1 [1]. We can choose, based on a particular application of interest, whether to represent these two-phase characteristics by a single or multiple attributes.

In the next four sections of this paper, we present trend detection methods based on fuzzy logic, statistical, regression, and wavelet techniques. In Section II-B, we propose a noise rejection fuzzy clustering approach for trend detection in physiological signals. We also review a fuzzy course approach for trend detection in Section II-A. In Section III, we review a statistical trend detection methodology based on Trigg's approach. In Section IV, we review a regression methodology for trend detection based on an original work presented in [1]. In Section V, we outline systematic steps involved in using wavelet decomposition techniques for detection of meaningful trends in physiological signals. Simulations that validate the effectiveness of the implemented trend detection methods will be presented in Section VI. A comparative study of the different trend detection methods is also presented in this section. Finally, the conclusions of this work will be given in Section VII.

II. Fuzzy Logic Methodologies in Trend Detection

In this section, we investigate two different fuzzy logic-based approaches for trend detection of time-series physiological data. Fuzzy approaches are introduced herein due to their 1) ability to identify underlying trends during high fluctuations of a signal; and 2) aptitude in the presence of noisy information. The first approach uses a time-dependent "fuzzy course" [2] to assess the compatibility of a signal with a predefined trend pattern. The second approach uses a noise-rejection fuzzy clustering algorithm to fit two clusters centers into a monitored time-series signal. The locations of those centers and the corresponding time stamps are used to identify the underlying trend and its shape.

A. Fuzzy Logic Course Approach

In this section, we present a fuzzy logic-based approach to trend detection that was initially introduced in [2]. The approach uses a time-dependant *fuzzy course* to define a certain trend of a variable. The trends in this case correspond to the patterns of the signal similar to those shown in Fig. 1. The compatibility of a sequence of samples with such a trend is then calculated to determine the occurrence or nonoccurrence of such a trend (in close to real-time mode). In other words, as shown in Fig. 2, a fuzzy course of a variable x: $W_c \rightarrow \delta_x$ with $\delta_x \subset \Re$ is specified by the function $\tilde{x} : W_c \rightarrow \tilde{\Re}$, where $\tilde{\Re}$ is the set of normalized and convex fuzzy subsets $\Re$, and W_c is the universe of discourse of variable x. Moreover, if $\tilde{x}(t)$ is a fuzzy course defined on the interval $[0, d]$, then a fuzzy trend $\tilde{G}_x$ (with $\Delta\tilde{G}_x = d$ as its duration) is defined in terms of $\tilde{x}(t)$ as [2]

$$\tilde{G}_x = \left\{ (g(t), \mu) \,|\, \mu = \inf_{t_0 \in [0,d]} \mu_{\tilde{x}(t_0)} g(t_0) \right\}. \quad (1)$$

In (1), $g(t)$ is a time-series course of a variable (starting at time instant t_0) that is being monitored for trend identification. The compatibility of a sequence of observations $\langle \mathrm{x}(t_1), \ldots, \mathrm{x}(t_m), \ldots \mathrm{x}(t_n) \rangle$ with the fuzzy trend in (1) is given by [2]

$$\wp[\langle \mathrm{x}(\mathrm{t}_1), \ldots, \mathrm{x}(\mathrm{t}_\mathrm{m}), \ldots \mathrm{x}(\mathrm{t}_\mathrm{n}) \rangle, \tilde{G}_x, t_\Omega] = \underset{t_m : t_\Omega < t_m \leq t_\Omega + \Delta\tilde{G}_x}{\mathrm{mean}} \left(\mu_{\tilde{x}(t_m - t_\Omega)} x(t_m) \right). \quad (2)$$

As shown in the example in Fig. 2, the compatibility of a sequence of samples with the fuzzy trend specified in (1) is determined by the smallest degree of membership of a sample $x(t_m)$ in the fuzzy course at time t_m. The above approach [through the use of the compatibility measure (2)] has the advantage of being least susceptible to high fluctuations in a signal during underlying trend identification.

B. Noise-Rejection Clustering for Trend Detection

In this section we propose a new fuzzy logic-based approach to trend detection. The proposed approach uses online noise-rejection fuzzy C-means (FCM) clustering to identify the different trends in a monitored variable. As a starting point for this algorithm, a simple and practical FCM clustering approach is proposed to partition the real-time single (or multi)-phase pattern of observations. The clustering algorithm possesses a noise rejection capability based on a criterion for assigning a cutoff distance for the noise in the data. The optimum number

of partitions corresponds to the minimum of the following cluster validity index

$$\mathrm{S_{cs}(U,V;X)} = \sum_{\mathrm{k=1}}^{\mathrm{N}} \sum_{\mathrm{i=1}}^{\mathrm{c}} (\mathrm{u_{ik}})^{\mathrm{m}} (\|\mathrm{x_k} - \mathrm{v_{ci}}\|^2 - \|\mathrm{v_{ci}} - \bar{v}\|^2) \quad (3)$$

where c is the number of clusters, N is the number of data, u_{ik} is the membership grade of data point x_k in cluster i, m is the degree of fuzziness (weight exponent), v_{ci} is the location of the cluster center, and $\bar{v}$ is the fuzzy total mean vector of the data that can be defined as

$$\bar{v} = \frac{1}{\sum_{\mathrm{i=1}}^{\mathrm{c}} \sum_{\mathrm{k=1}}^{\mathrm{N}} (\mathrm{u_{ik}})^{\mathrm{m}}} \sum_{\mathrm{i=1}}^{\mathrm{c}} \sum_{\mathrm{k=1}}^{\mathrm{N}} (\mathrm{u_{ik}})^{\mathrm{m}} \mathrm{x_k}. \quad (4)$$

For the selection of the weight exponent that defines the degree of fuzziness, we use the following fuzzy total scatter matrix [12]

$$S_{\mathrm{T}} = \sum_{k=1}^{\mathrm{N}} \left(\sum_{\mathrm{i=1}}^{\mathrm{c}} (\mathrm{u_{ik}})^{\mathrm{m}} \right) (\mathrm{x}_k - \bar{v})(\mathrm{x}_k - \bar{v})^{\mathrm{T}}. \quad (5)$$

In the above equation, the trace of the fuzzy scatter matrix decreases monotonically from a constant value J to zero as the degree of fuzziness increases. It is recommended to select the level of fuzziness m such that the trace of the scatter matrix is $0.5J$ [14]. An agglomerative hierarchical clustering algorithm [13] is suggested to identify the initial centers v_{hi}. Next, to find the data points that are "far" from all clusters, we use [14]

$$W_k = \sum_{i=1}^{c} \|x_k - v_{hi}\|_A \quad (6)$$

where $j = 1, 2, \ldots, N, c$ is the number of clusters, N is the number of data, and v_{hi} is the estimate center of cluster i obtained by the AHC algorithm. The index W_k gives a measure of how far each data point is from the different cluster centers assigned in the first step of the algorithm. The noise is identified through the data points that have large values of W_k and, therefore, a threshold Ω is assigned to trim these outliers from the data set. After choosing the threshold, the following ratio is computed:

$$\delta = \frac{\eta_n}{N} \quad (7)$$

where η_n is the number of noise points and N is the total number of data. The percentage of "good" gain values, i.e., inliers can then be calculated as

$$\hat{\delta} = (1 - \delta). \quad (8)$$

Then, we calculate the cutoff distance [14]

$$u^2_{\mathrm{FC_{cut}}} = g_{\mathrm{i}} \chi^2 \quad (9)$$

where g_i is a resolution parameter often selected in the range of 0.2–0.45 [14]. The chi-square value χ^2 is selected for a single degree of freedom as 0.95 assuming that 95% of the observations in the signal are inliers. Finally, we calculate the membership matrix using [15]

$$\mathrm{u_{ik}} = \frac{1}{1 + \left\{ \frac{u^2_{\mathrm{FC_{cut}}}(\mathrm{x_k}, v_{\mathrm{hi}})}{g_{\mathrm{i}}} \right\}^{\frac{1}{\mathrm{m}-1}}}. \quad (10)$$

In specific terms, we can detect different trends in a monitored signal using the clustering approach proposed above as shown in Fig. 3. For example, if the variable of interest is monotonically increasing, we can set the cluster validity index in (3) as $S_{cs} = 2$ and compute the location of the cluster centers $v_{ci}(i = 1, 2) = (v_{c1}, v_{c2})$. Then, we can identify the "increase" trend through the following fact:

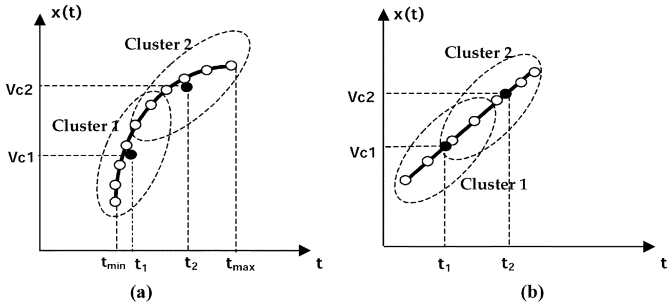

Fig. 3. identification of a trend based on fuzzy c-means clustering.

$$v_{c2} > v_{c1}. \quad (11)$$

Also, in this case, the type of increase "monotonic" is detected from the velocity of the signal during the trend duration if

$$\frac{\partial x(x_i \,|\, v_{c1} < x < v_{c2})}{t_2 - t_1} > 0. \quad (12)$$

And the acceleration of the signal during the trend duration must satisfy

$$\frac{\partial \partial x(x_i \,|\, v_{c1} < x < v_{c2})}{(t_2 - t_1)^2} < 0. \quad (13)$$

Moreover, if the type of increase is "linear," then

$$\frac{\partial \partial x(x_i \,|\, v_{c1} < x < v_{c2})}{(t_2 - t_1)^2} \approx 0. \quad (14)$$

A similar approach can be adopted for every type of pattern in Fig. 1. In summary, the type of the trend (increase, decrease, etc.) is determined automatically using noise-rejection fuzzy clustering and based on the location of the clusters centers. The trend is identified from the velocity and acceleration of the signal between the calculated clusters centers (similar to analysis in (11)–(14). In later sections of this paper, we present simulation results that implement the preceding two fuzzy trend detection methods for real-time monitoring of meaningful variations in physiological signals.

III. Trigg's Statistics-Based Trend Detection Algorithm

The Trigg's trend detection approach is a statistical method that monitors the variation of a signal in real time (or pseudo real time) using a tracking variable T. The Trigg's tracking variable T is a signal detection index which assigns a value between -1 and $+1$ to the likelihood that a trend is occurring. At $\mathrm{T} = +1$ there is 100% certainty the variable is rising, and at -1 there is 100% certainty the variable is falling. The T variable is calculated using the difference between the current value of the variable and time weighted moving average of the previous values [9]. The description of the calculation of the Trigg's tracking variable T is adopted from Hope *et al.* [10].

The initialization of the algorithm requires a value of the signal at the beginning of the monitoring window $\bar{\phi}$. The weighted average of the first sampling period is

$$u_{t(0)} = \bar{\phi} \tag{15}$$

and the prediction error of the samples in the monitoring time interval can be defined as

$$s_{t(0)} = \frac{\bar{\phi}}{100}. \tag{16}$$

Also, the initial mean absolute deviation in the monitoring time interval can be approximated by

$$M_{t(0)} = \frac{\bar{\phi}}{10}, \tag{17}$$

Therefore, as we assess the trend (in a feedforward manner) in a set of samples of a signal in a monitoring time window, the prediction for an upcoming sample can be defined as

$$u_t = \vartheta d_t + (1-\vartheta)u_{t-1} \tag{18}$$

where d_t is the current value of the signal, u_{t-1} is the prediction at the previous time sample, and ϑ is a design parameter between 0 and 1, which determines the time constant of the exponential weighting (usually 0.1–0.22 [10]). Therefore, the error in prediction of the current value is

$$e_t = d_t - u_{t-1} \tag{19}$$

and this error signal can be redefined using the following:

$$s_t = \vartheta e_t - (1-\vartheta)s_{t-1}. \tag{20}$$

Then, the mean absolute deviation for the current time instant is defined as

$$M_t = \vartheta|e_t| + (1-\vartheta)M_{t-1}. \tag{21}$$

From (21), the Trigg's tracking index T is calculated as

$$T_t = \frac{s_t}{M_t}. \tag{22}$$

Finally, the statistical variables are updated as follows:

$$u_{t-1} = u_t$$
$$s_{t-1} = s_t$$
$$M_{t-1} = M_t.$$

The T index in (22) can be used to determine and track a trend in a signal variable through real-time monitoring, i.e., instant-by-instant assessment of the signal. Moreover, the above algorithm can also be used to identify trends in a signal being monitored over short durations of time (using a monitored window). In such case, the status of the trend is identified using

$$T = \frac{\sum_{t=1}^{\rho} T_t}{\rho} \tag{23}$$

where ρ is the overall number of samples or observations of the signal. The index in (23) is always a value between -1 and $+1$ that determines the likelihood that a trend is occurring. At $+1$, there is 100% certainty the variable in the monitoring window is rising. At -1, there is 100% certainty the variable is falling. Examples for the use of the Trigg's approach to detect trends in physiological signals, i.e., heart beat rate will be given in the simulation section of this paper.

IV. Regression and Temporal Shape Trend Analysis

In [11], a generic methodology for qualitative analysis of temporal shapes of a continuous variable was proposed. Such methodology would be suitable for the detection of various trends in physiological signals because of its generality and lack of dependence on dedicated templates that need to be defined for every monitored variable *a priori*. Furthermore, unlike the Trigg's algorithm the temporal shape algorithm reviewed in this section has the capability of efficiently identifying the shape of the trend being monitored. The approach consists of three main phases: 1) analytical approximation of the variable; 2) its transformation into a symbolic form based on the signs of the first and second derivatives of the analytical approximation function; and 3) degree of certainty calculation. At the first step, the process variable $x_j(t)$ is approximated by

$$x_j^*(t) = c_0 + c_1 t + c_2 t^2 + \cdots + c_m t^m \quad t \in [t_1, t_2] \tag{24}$$

where m is the order of the polynomial and $c_k (k = 1, \ldots, m)$ are the unknown coefficients. To speed up the real-time computation, the following approximation equation is used

$$H^T \cdot H \cdot \{c\} = H^T \cdot \{x\} \tag{25}$$

where the matrix H is defined as shown in (26) at the bottom of the page. In (26), $[t_1 + (n-1)\cdot\Delta T] = t_2$ and ΔT is the sampling interval. By setting $t_1 = 0$ and $\Delta T = 1$, matrix H can be calculated *a priori* knowing the polynomial order and the length of the discrete time interval. Hence, the polynomial coefficients can be solved using

$$\{c\} = (H^T \cdot H)^{-1} \cdot H^T \cdot \{x\} = Q \cdot \{x\} \tag{27}$$

where Q is a constant matrix. At the second step, feature strings are extracted from the analytical approximation function in (24). The extraction of a sequence of signs is described by the following operators (L1 for velocity, and L2 for acceleration):

$$L1[x_j^*(t)] = \mathrm{sd1}(+, -, \cdots, +) \quad t \in [t_1, t_2] \tag{28}$$
$$L2[x_j^*(t)] = \mathrm{sd2}(+, -, \cdots, +) \quad t \in [t_1, t_2]. \tag{29}$$

Where sd1 is the sign of the difference between every sample and the proceeding one in the velocity signal of the process variable in (24), i.e., $L1$. Also, sd2 is the sign of the difference between every sample and the proceeding one in the time derivative of the process variable velocity of (28). Some simple patterns (similar to those in Fig. 1) can be adequately represented by

$$H = \begin{bmatrix} [t_1 + 0\cdot\Delta T]^0 & [t_1 + 0\cdot\Delta T]^1 & \cdots & [t_1 + 0\cdot\Delta T]^m \\ [t_1 + 1\cdot\Delta T]^0 & [t_1 + 1\cdot\Delta T]^1 & \cdots & [t_1 + 1\cdot\Delta T]^m \\ \vdots & \vdots & \ddots & \vdots \\ [t_1 + (n-1)\cdot\Delta T]^0 & [t_1 + (n-1)\cdot\Delta T]^1 & \cdots & [t_1 + (n-1)\cdot\Delta T]^m \end{bmatrix} \tag{26}$$

$L1$ and $L2$. The qualitative shape of the process variable is represented by combining the strings in (28) and (29). In other words

$$q\,\text{shape}[x_j(t)] = L1[x_j^*(t)]; \quad L2[x_j^*(t)] = (+,-,\cdots,+);(+,-,\cdots,+). \tag{30}$$

The degree of compatibility is calculated through the following formula:

$$\text{dc} = \text{cmp1}(\text{sd1}, \text{sd1}^L)\left(1 - k_1\frac{\text{cmp2}(\text{sd2}, \text{sd2}^L)}{R} - 0.5k_2\right) \tag{31}$$

where k_1 and k_2 are positive constants. Also $\text{cmp1}(\text{sd1}, \text{sd1}^L)$ is defined as

$$\text{cmp1}(\text{sd1}, \text{sd1}^L) = \begin{cases} 0 \rightarrow \text{sd1} \neq \text{sd1}^L \\ 1 \rightarrow \text{sd1} = \text{sd1}^L \end{cases}$$

and $\text{cmp2}(\text{sd2}, \text{sd2}^L)$ gives the relative number of symbols in the second derivative string that do not match. Examples for the use of the above approach to detect trends in synthetic physiological signals will be given in the simulation section of this paper.

V. Wavelet-Based Trend Detection Approach

Often a particular spectral component occurring at any instant can be of particular interest. In these cases it may be very beneficial to know the time intervals these particular spectral components occur. For example, in EEGs, the latency of an event-related potential is of particular interest (Event-related potential is the response of the brain to a specific stimulus like flash-light, the latency of this response is the amount of time elapsed between the onset of the stimulus and the response). Wavelet transform is capable of providing the time and frequency information simultaneously, hence giving a time-frequency representation of the signal. In other words, with Fourier transformation (FT), the frequency and time information of a signal at some certain points in the time-frequency plane cannot be known. In other words, we cannot know what spectral component exists at any given time instant. The best we can do is to investigate what spectral components exist at any given interval of time. This is a problem of resolution, and it is the main reason why researchers have switched to wavelet transform (WT) from Fourier transform (FT). short-time FT gives a fixed resolution at all times, whereas WT gives a variable resolution. Therefore, wavelet-based signal processing methods have been recently gaining popularity for feature extraction.

In [7], a wavelet theory-based nonlinear adaptive system for identification of trends from sensory data was developed. In [8], the authors applied wavelet-based approach to identification and localization of polynomial trends in noisy measurements. Their method yields both the least squares polynomials for the identified intervals and a quantitative measure for their goodness of fit.

In practical applications, wavelet can be used to visualize an underlying trend in a noisy signal [11]. The shape of such trend might not be apparent upon visual inspection of the original signal. In this paper, we implement a multilevel wavelet decomposition of a monitored signal by passing it through a series of filters, i.e., low-pass, high-pass, etc. As a result of this process, the underlying trend becomes clearer and clearer with every pass (decomposition). This is due to the fact that the trend represents the slowest part of a monitored signal. In wavelet analysis, this corresponds to the greatest scale value. As the scale increases, the resolution decreases, thereby producing a better estimate of an unknown trend. Once the trend becomes visible, temporal reasoning can be used on the velocity and acceleration of the decomposed signal to determine whether the variable is rising or falling (as defined in the previous sections), i.e., describe the visible trend.

VI. Simulation and Comparison of Trend Detection Methods

In this section, we present numerical simulations to show the performance of the various trend detection approaches used to monitor physiological signals. We used experimentally collected systolic blood pressure and heartbeat rate, and synthesized opacity signals to validate the effectiveness of the implemented trend analysis techniques. The trend detection algorithms are all implemented in Matlab 6 simulation environment. The techniques were investigated with various user-defined monitoring durations. The monitoring windows for the various experiments are set as either short-term or long-term duration. This selection depends on the requirements of monitoring being either short or long term signal detection, e.g., ambulance electrocardiography (ECG) diagnosis versus Holter ECG or sleep ECG. In general, short-term monitoring is used to capture trends in signals with fast varying dynamics and meaningful short duration variations. Long-term monitoring on the other hand is recommended for signal with slow-varying base frequencies that embody a meaningful trend in a longer monitoring duration. Therefore, we tested the various trend detection algorithms for both types of monitoring duration to assess their effectiveness in extracting trends with both slow and fast frequency components. Furthermore, we adopted a continuity criterion to associate consecutive monitoring time windows. In other words, consecutive monitoring windows can overlap each other or be completely distinct. Short-period overlapping monitoring windows are recommended for continuous monitoring in order to ensure that the overall dynamics performance of the signal is examined and all meaningful trends are captured. On the other hand, nonoverlapping time windows are used when continuous monitoring is not a necessity or if a signal is being monitored for trends periodically but at no continuous intervals. Therefore, we tested the various trend detection algorithms for windows with both criteria to assess their effectiveness in extracting trends in continuous or discontinuous (periodic) monitoring.

We start with the presentation with the evaluation of the fuzzy course approach presented in Section II-A. For this purpose, we use a typical systolic blood pressure signal. Fig. 4(a) shows an interpolated version of the signal resampled at 100 Hz using

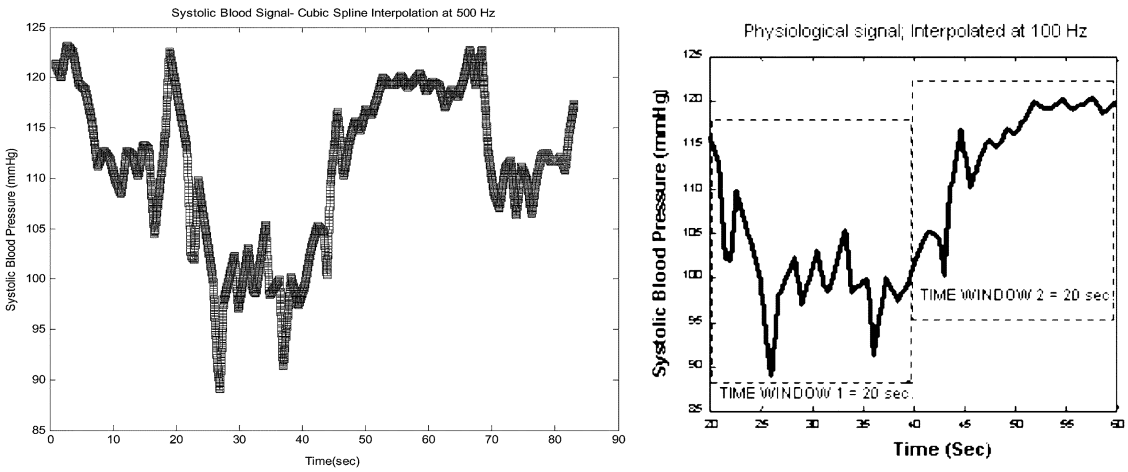

(a) (b)

Fig. 4. (a) Systolic blood pressure signals used in testing the fuzzy noise-rejection trend detection example, and (b) a 40-s-long (2 monitoring windows; 20 s/window) portion of the interpolated systolic blood pressure signal in Fig. 4(a) (used in testing the fuzzy course trend detection approach).

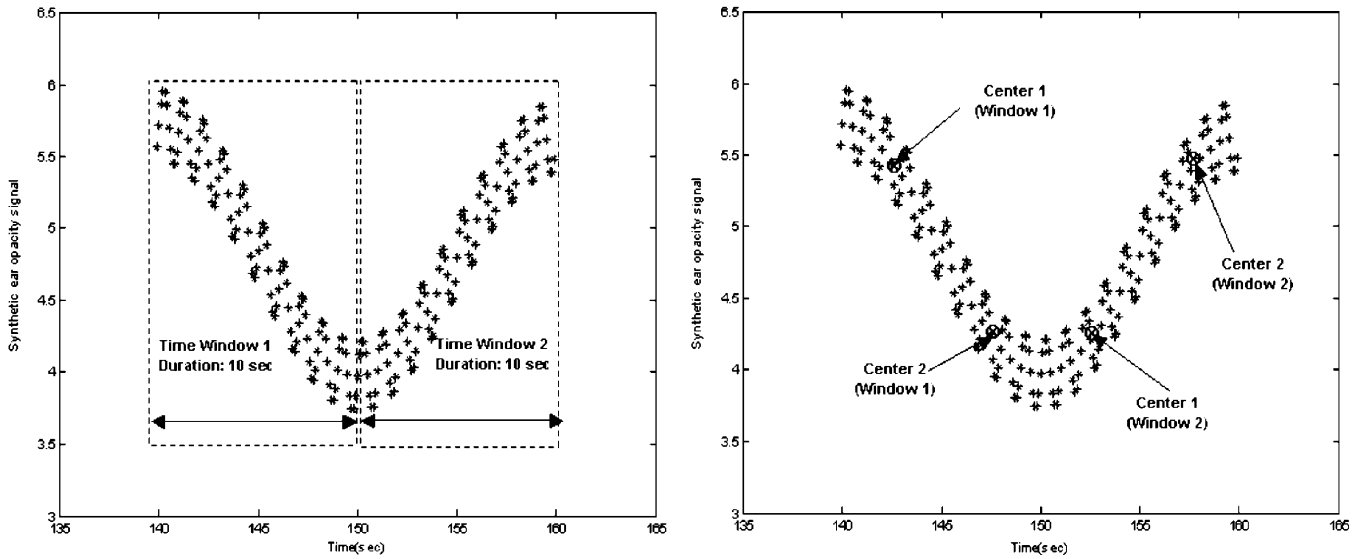

(a) (b)

Fig. 5. (a) A 20-s-long portion of a synthetic ear opacity signal used in testing the noise-rejection fuzzy trend detection approach, and (b) location of the cluster centers in the noise-rejection fuzzy trend detection approach.

cubic spline techniques (in MATLAB 6.5 environment). Interpolation is used to fill missing data points from the original physiological signal. The original signal obtained from experimental data is 83 s in duration. In this analysis we select time monitoring windows of 20-s duration. In specific terms, Fig. 4(b) shows a 40-s segment of the interpolated systolic blood pressure signal in Fig. 4(a). Using such segment, we implement the fuzzy course approach to assess the status of the underlying trend twice in 40 s (two monitoring windows; each one is 20 s in duration). During the analysis, the fuzzy course approach showed a satisfactory accuracy and speed in analyzing the underlying trend in the monitored signal. The approach correctly identifies the trend status for each of the two monitoring windows as "monotonic variable decrease/concave upward" and "monotonic variable increase/concave downward."

In the second set of experiments, we evaluate the fuzzy noise-rejection method for trend detection presented in Section II-B. Fig. 5 shows a 30-s-duration portion of a synthetic ear opacity signal used to test the trend detection approach. The approach in Section II-B is used to monitor 10-s-long segments of a 20-s portion of the signal as shown in Fig. 5(a). Upon implementation, the proposed approach correctly identified the trend status in both segments as "monotonic variable decrease/concave downward" and "monotonic variable increase/concave downward." The locations of the computed fuzzy clusters centers are shown in Fig. 5(b). In this example, real-time trend detection involves setting the monitoring interval to 10 s, which meant that two consecutive nonoverlapping monitoring windows are needed to track the ear opacity signal being studied. Above process is repeated for as long as the signal monitoring is required.

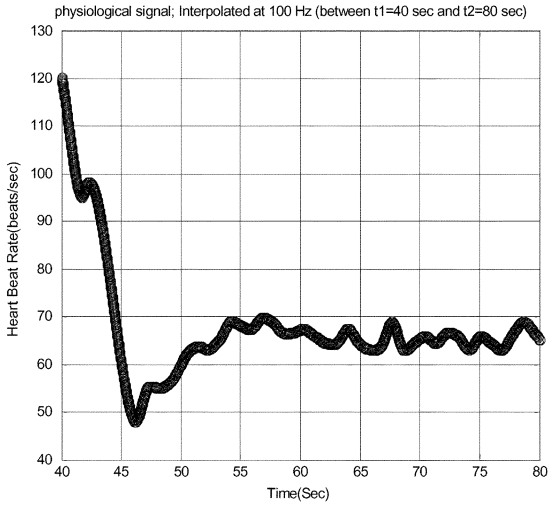

Fig. 6. The 40-s-long PB signal.

In the third set of examples, we evaluate the Trigg's statistical trend detection approach proposed in Section III of this paper. We selected a heartbeat rate signal to validate the effectiveness of the proposed approach in detecting trends in the signal for the monitoring duration. The original signal obtained from experimental data has 180 s in duration. A cubic spline of the original signal resampled at 100 Hz in MATLAB 6.5 is considered to populate the 180-s duration signal with more continuous observations. This interpolated heartbeat rate variable is used in the evaluation of the Trigg's trend detection method and a monitoring window of 40-s duration is selected to continuously monitor the signal. Fig. 6 shows the monitoring window considered, which starts at the 40th s and has 40 s in duration. Fig. 7 shows the following outcome of the implementation of the Trigg's (statistical) trend detection approach: the prediction error of the Trigg's index T [Fig. 7(a)]; the smoothened prediction error [Fig. 7(b)]; and the T index tracking the original signal [Fig. 7(c)]. Using the T index in (23), the approach identified the signal as decreasing over the 40-s monitoring interval, i.e., mean $\mathrm{T} < 0$.

In the fourth set of examples, we evaluate the regression trend detection approach proposed in Section IV of this paper. We selected both a synthetic opacity and a real heartbeat rate signals to validate the effectiveness of the proposed approach. First, for the synthetic opacity signal, a monitoring window of 500-s duration is selected for continuous monitoring. Fig. 8 shows a synthetic opacity signal used to test the regression/temporal shapes trend detection approach. In the first run, we selected a monitoring window of 500 s (which is equal to the duration of the entire signal). A third-order polynomial fit of the opacity signal monitored is also plotted in Fig. 8 to smoothen the signal for monitoring low-frequency underlying trends. A second or third-order polynomial fit is sufficient for such signal since the underlying trend in 500 s has a half-parabola single-phase pattern. Despite the profound ear opacity pulse oscillations, which simulates the phenomena typically observed in G exposures, the trend detection algorithm accurately outputs the overall trend status over the 500-s-long monitoring interval (based on temporal analysis of the third-order polynomial fit). In the second run, we analyzed a small portion of the synthetic opacity signal in order to validate the effectiveness of the temporal trend detection approach in both short and long-term monitoring. In specific terms, a 30-s-long segment of the same signal is considered. To accurately detect the underlying trend, the monitoring window for the 30-s segment is set to 15 s. The third-order polynomial fit curves for both segments of the signal are shown in Fig. 9. Based on temporal analysis of a third-order polynomials fit, the algorithm accurately outputs the trend status for both the 15-s-long monitoring windows.

Second, we selected a heartbeat rate signal similar to that shown in Fig. 4 to validate the effectiveness of the proposed approach for detecting trends in both synthetic and actual physiological signals. A monitoring window of 5-s duration is selected to continuously monitor the signal. The interpolated heartbeat rate signal is a "cubic spline" of the original signal resampled at 100 Hz. Fig. 10 shows a 20-s segment of the heart beat rate signal in Fig. 7(a); to be used for testing the trend detection approach. We set the monitoring window to 5 s. Fig. 11 shows the fifth-order polynomial fit curve to each of the segments of the heart rate signal. Using those polynomial fit curves, the trend detection approach correctly identified the status and the shape of the trend in each of the four segments of the signal.

In the last set of examples, we evaluated the wavelet-based trend detection approach. For this purpose, we use a synthetic opacity signal. The wavelet approach is implemented through the following steps: 1) performing a 3-level decomposition on the signal of interest due to the presence of noise that overrides the underlying trend; 2) identifying the first level of decomposition, that most likely embodies the underlying trend; and 3) implementing temporal reasoning to identify trends in the first-level decomposition of the original signal. We used the entire 500-s signal in Fig. 8, and we set the duration of monitoring window to 250 s. Fig. 12(a)–(b) shows the first-level wavelet decomposition of the first and second 250-s segments of the synthetic opacity signal, respectively. The higher frequencies, and noise in the original signal do subside significantly in the first-level wavelet decomposition. It is also concluded from this analysis that the wavelet decomposition strategy can extract an underlying trend from a noisy signal, or a signal with multiple frequency components. The status of such trend can be assessed using templates similar to those in Fig. 1.

Furthermore, we performed additional numerical simulations to directly compare the performance of the proposed trend detection approaches when used to monitor some the typical physiological signals studied, thus far. Moreover, the analysis presented here is used to infer knowledge and recommendations on how to choose most suitable approaches for monitoring specific physiological signal(s) of interest. The additional comparative examples presented below were selected to cover various situations representative of noisy signals with different levels of frequencies.

For the first example, we selected a medium-size monitoring window for trend detection in systolic blood pressure signals. As the width of the monitoring window increases, the frequency of the noise becomes noticeably larger. On the contrary, as the duration of monitoring decreases, the frequency of the signal fluctuations becomes noticeably smaller. This phenomenon becomes more evident in the second example, where the duration of the monitoring segment is longer (60 s) during trend detection of a heartbeat rate signal. Finally, in the third example, we used

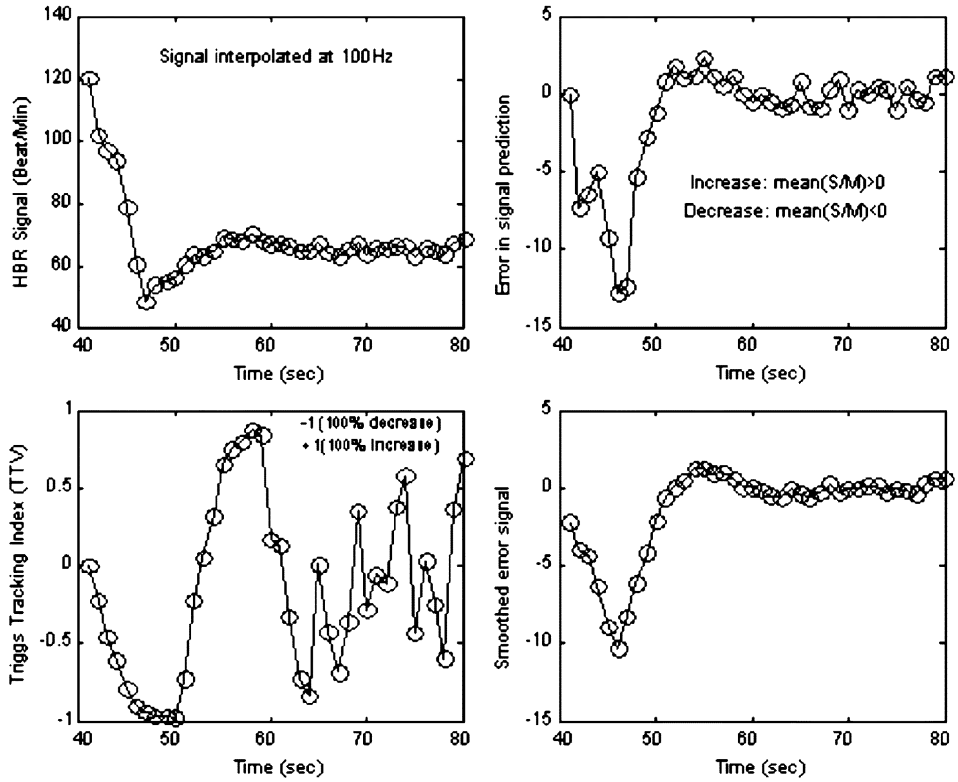

Fig. 7. Output of the Trigg's (statistical) trend detection approach: (a) top-left: the signal being monitored; (b) top-right: prediction error of the TTV index; (c) bottom-right: the smoothened prediction error; and (d) bottom-left: TTV index tracking the original signal.

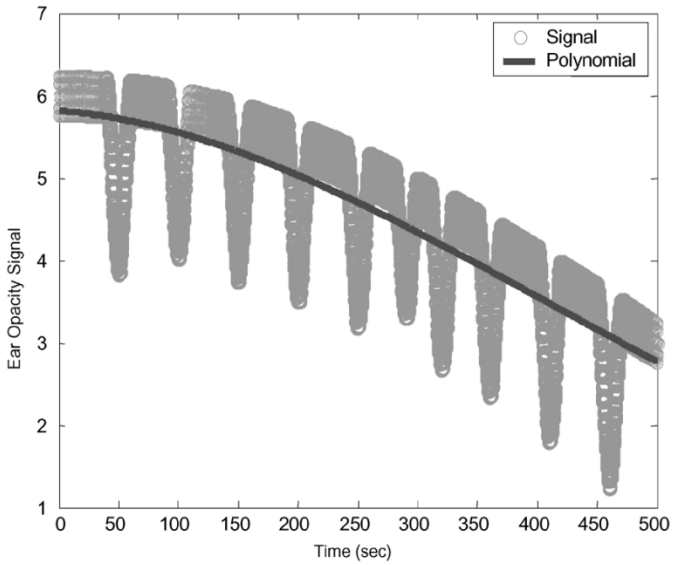

Fig. 8. Synthetic opacity signal and the third-order polynomial fit to the 500-s-long signal.

a short duration monitoring windows for an opacity signal with very high-frequency noise that overrides the underlying trend. In this sense, each of the examples used to compare the various developed trend approaches presents a distinct noise (or signal fluctuations) frequency versus monitoring window width relation.

In the first comparison we use the blood pressure signal shown in Fig. 4. The portion of the signal under observation is 89 s in duration. The sampling frequency is 1 Hz. We wish to identify trends in the signal using nonoverlapping segments each of 44-s to 45–s duration. For the portion of the signal considered this breakdown maps into two segments as shown in Fig. 13. For the purpose of detecting meaningful trends in every segment we apply the five approaches developed in this paper.

We intuitively specified the linguistic description of the shape of the trend as the most important criterion in evaluating the different detection approaches. In specific terms, to evaluate the accuracy of a specific trend detection technique we assess: 1) the ability of the approach to identify the trend, i.e., increase, decrease, etc., and 2) the ability of the approach to identify the shape of the trend, i.e., monotonic increase, linear decrease, etc. The correctness in identifying a trend (or its shape) is determined through comparison with the actual signal trend identified by visual inspection in each monitoring segment. The evaluation criterion specified herein is indeed compatible with those of the fuzzy noise-rejection approach (11)–(14) and the regression approach (30)–(31). In general, in the majority of monitoring applications it is the status of the signal trend that matters the most whereas accuracy in the description of its shape is less critical. For trend detection in the signal of Fig. 13, the comparison results of all five approaches are summarized in Table I. The last column of Table I lists the computation time required for every algorithm. The computation time depends on the speed of the processing microchip. Speed of computation is an important parameter to consider for real-time monitoring purposes. In our comparison tables, the computation times of the trend detection algorithms are reported to give a better indication of the speed of processing of every algorithm relative to the other four. In the current example, by visual inspection we identify a trend decrease and a shape of concave down

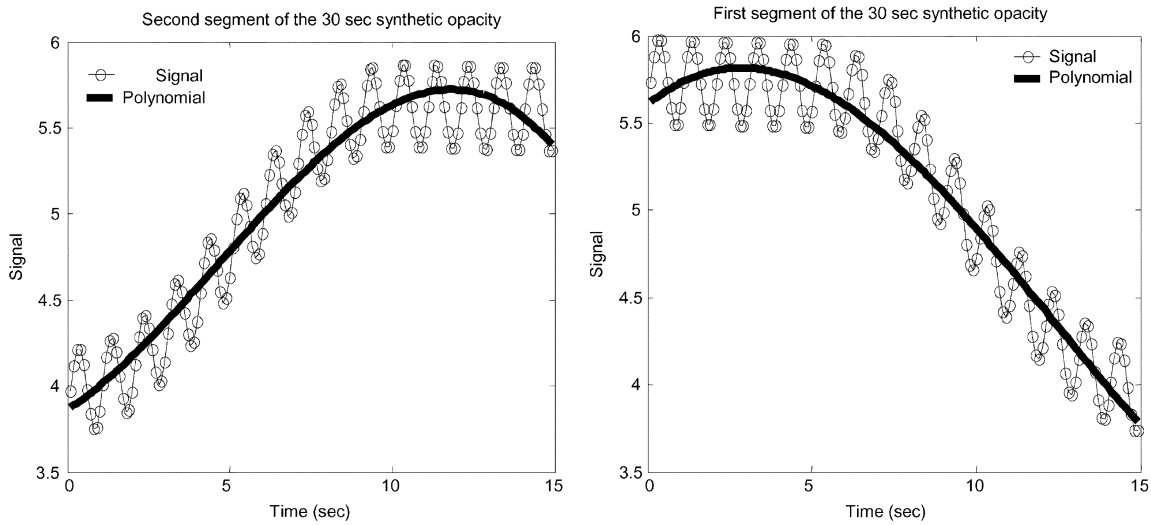

Fig. 9. Third-order polynomial fit to each of the 15-s-long segments of the opacity signal used for testing the regression/temporal shapes trend detection approach.

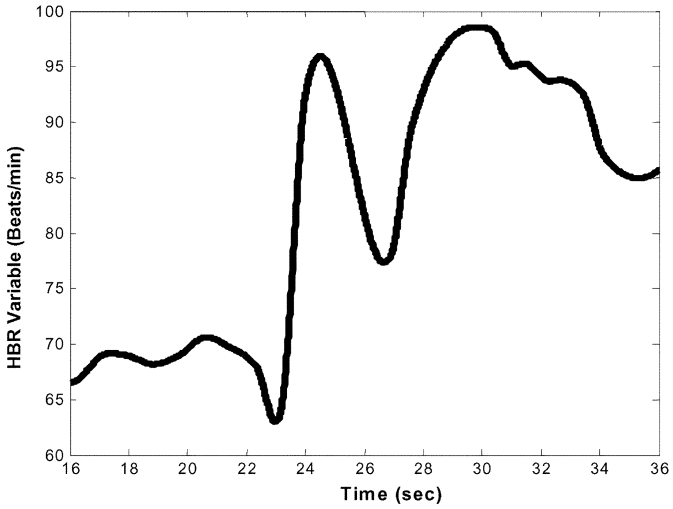

Fig. 10. A 20-s-long segment of the heartbeat rate signal in Fig. 7(a) used for testing the regression/temporal shapes trend detection approach.

in segment 1 of the signal. Furthermore, we identify a trend increase and a shape of concave upward in segment 2 of the signal. Those are set as "gold standard" and the various trend detection approaches are evaluated based on how close their detection matches such visual observations. As seen from the results, all the proposed trend detection approaches correctly identified the trend in each of the two segments of the 60-s signal portion being monitored. However, the accuracy in identifying the exact shape of the trend varies from one approach to another. In specific terms, the fuzzy noise-rejection, and the fuzzy course approaches correctly identified the shape of the trend (concave upward) only in the first segment. In the second segment, however, the shape of the trend is extremely difficult to detect simply because the segment has a two-phase pattern. The wavelet decomposition approach correctly identified the shape of the trend (concave upward) only in the second segment of the signal. This is due to the fact that even after wave decomposition in the first segment was applied, the noise was still persistent. Hence, the second derivatives of the decomposed signal did not give an accurate shape of the trend.

The Trigg's statistical approach is not equipped with the capability of identifying shapes of the trends and hence received 'x' evaluation in this category. However, this statistical approach accurately identified the signal trends in each of the 30-s monitoring segments. Finally, the temporal reasoning approach proved to be the most accurate trend detection method for this specific example as it correctly identified the trends and their shapes in both the 44-s segments. The temporal reasoning approach showed such consistent behavior due to the fact that a fifth-order polynomial fit to the signal in both segments was smooth enough in a sense that its first and second derivatives gave an accurate indication of the trends and their shapes.

In the second comparison study we use a portion of the heartbeat rate signal shown in Fig. 6. The portion of the signal used in the comparison is about 180 s in duration. We wish to identify the trends in the signal using segments of ~ 58 s in duration. We also wish to perform continuous monitoring, hence every segment has a 5-s overlap with the preceding and proceeding signals, respectively. For the portion of the signal considered, this breakdown maps into 3 overlapping segments as shown in Fig. 14. For the purpose of detecting meaningful trends in every segment we implemented each of the five approaches outlined in this paper. By visual inspection of Fig. 14, we can define the following: 1) a trend *decrease* and a shape *concave upward* in segment 1 of the signal; 2) a trend *increase* and a shape *concave upward* in segment 2 of the signal; and 3) a trend is *constant*, and heartbeat rate is almost unchanged overall in segment 3. The comparison results for all five trend detection methods are summarized in Table II. As evident from the comparison, most of the proposed techniques correctly identified the trend in each of the three segments of the 180-s-long signal. However, the accuracy in identifying the exact shape of the trend varies from one approach to another. In specific terms, the fuzzy noise-rejection approach correctly identified the shape of the trend in all three segments hence demonstrating consistent accuracy throughout. This is due to the fact that such approach is very immune to the high-frequency of the signal fluctuations. On the other hand, the fuzzy course approach did not identify the shape of the trend in the first segment of the signal. This is attributed to the fact that the shape of the trend in the first segment is

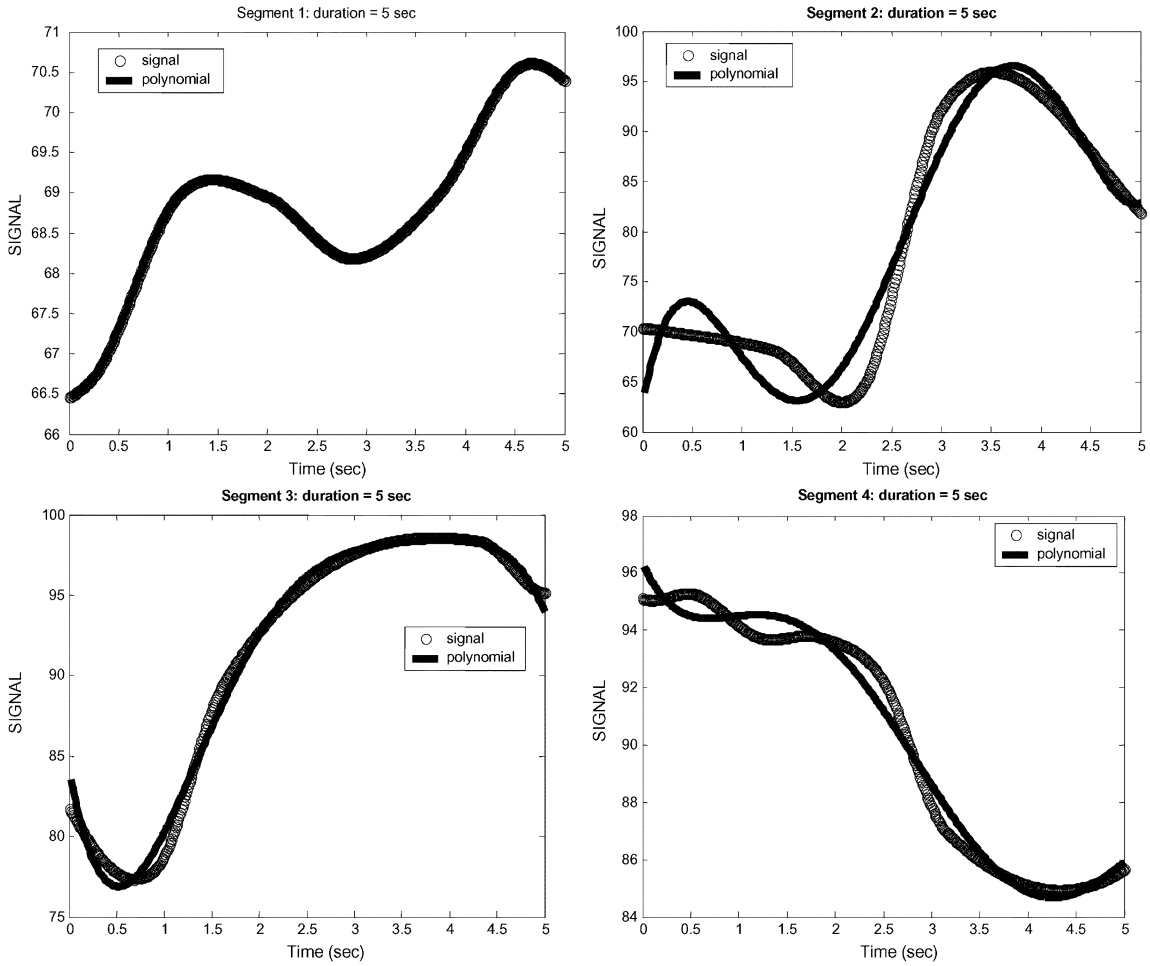

Fig. 11. Fifth-order polynomial fit to each of the 5-s–long segments of the heartbeat rate signal used for testing the regression/temporal shapes trend detection approach.

difficult to detect simply because of the presence of a two-phase pattern. The Trigg's statistical approach accurately identified the signal trends in the first two segments but failed to identify that the signal is (almost) unchanged in the third segment. This is due to the long duration of monitoring (as opposed to minimum amplitude variation) whereas the approach is best suited for short duration monitoring (as in Table II). Moreover, the temporal reasoning approach correctly identified the trend and its shape for the first two segments but scored minimum weights through out for the last segment. Finally, the wavelet decomposition approach showed inconsistent accuracy during the 180-s duration of monitoring. In specific terms, the approach correctly identified the trend in the first two segments only. The shape of the trend was correctly identified in the first segment but not in the middle one. Such inconsistency can often be reduced or eliminated if higher-order decomposition is considered.

In the third comparison study, we used the 30-s portion of a synthetic opacity signal shown in Fig. 5. The portion of the signal under observation is about 20 s in duration. We wish to identify short-duration trends ($\sim$10 s) in the signal using segments of 10 s in duration. In addition, we chose not to track the trend continuously in order to test the effectiveness of the trend detection algorithm in handling nonoverlapping window monitoring intervals. Hence for the portion of the signal considered, this breakdown can map into two nonoverlapping segments as shown in Fig. 15. By visual inspection, we identify a trend *decrease* and a shape *concave upward* in segment 1 of the signal. Furthermore, we identify a trend *increase* and a shape *concave upward* in segment 2 of the signal. The comparison results for all five approaches are summarized in Table III. As seen from the results, all the proposed trend detection approaches correctly identified the trend in each of the two segments monitored. Also, the fuzzy course, the temporal reasoning, and the fuzzy noise-rejection approaches correctly identified the shape of the trend in both segments hence demonstrating full accuracy. This is attributed to the fact that the accuracy of all three approaches was least affected by the high-frequency noise overriding the signal in both segments of monitoring. The Trigg's statistical approach accurately identified the signal trends in both monitored segments, but it does not resolve the issue of a trend shape. Finally, the wavelet decomposition approach correctly identified the trend in both segments. However, the approach was not consistent in identifying the shape of the trend for either of the two segments. Again, this is due to the fact that the wave decomposition has eliminated very little of the high-frequency noise.

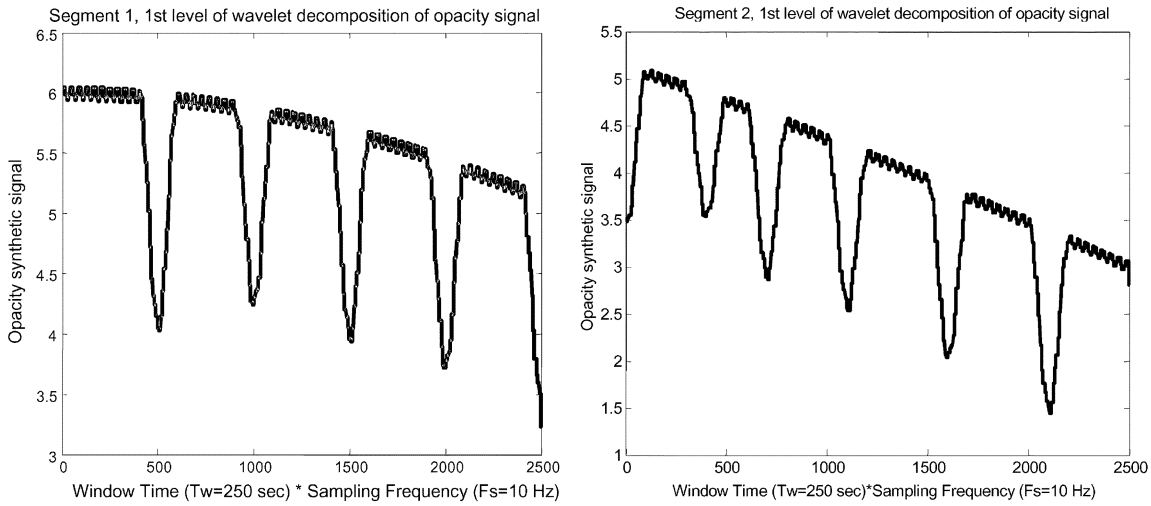

Fig. 12. (**a**) First-level wavelet decomposition of the first segment of the synthetic opacity signal in Fig. 10, and (b) first-level wavelet decomposition of the second segment of the synthetic opacity signal (250 s).

TABLE I
COMPARATIVE PERFORMANCE RESULTS FOR THE FIVE TREND DETECTION APPROACHES WHEN USED TO IDENTIFY TRENDS IN BP SIGNAL SHOWN IN FIG. 13

APPROACH (NON-OVERLAPPING WINDOWS IN SYSTOLIC BLOOD PRESSURE SIGNAL)	**TREND/SHAPE** (BY VISUAL INSPECTION) **Seg1: decrease, concave upward Seg2: increase, concave upward**	**TREND DETECT**	**SHAPE DETECT**	**COMPUTATION TME** (IN MATLAB 6 ENVIRONMENT)
Fuzzy Noise-rejection	Seg1: decrease, concave upward	√	√	3 seconds
	Seg2: increase, concave down	√	×	
Fuzzy Course	Seg1: decrease, concave upward	√	√	2 seconds
	Seg2: increase, linear	√	×	
Trigg's Statistical	Seg1: decrease	√	×	3 seconds
	Seg2: increase	√	×	
Temporal Reasoning	Seg1: decrease, concave upward	√	√	5 seconds
	Seg2: increase, concave upward	√	√	
Wavelet Decomposition	Seg1: decrease, linear	√	×	1 second
	Seg2: increase, concave down	√	√	

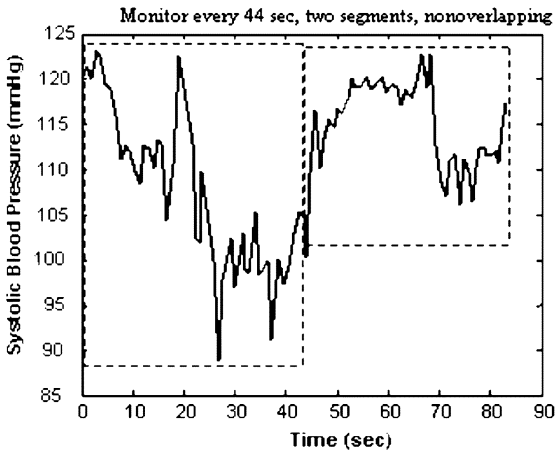

Fig. 13. The blood pressure signal considered in the first comparative analysis.

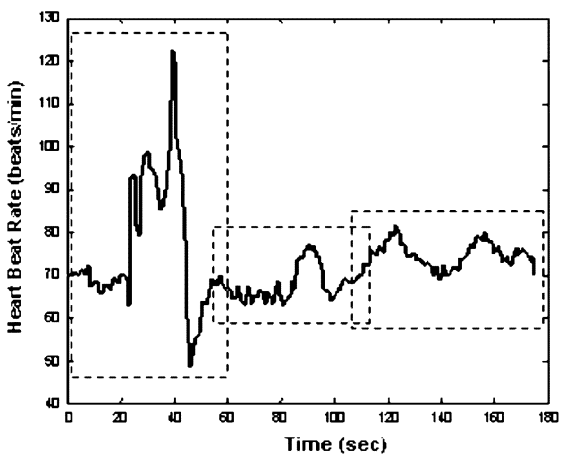

Fig. 14. The heartbeat rate signal considered in the second comparison.

VII. CONCLUSION

In this paper, we implemented and investigated various fuzzy-logic, statistical, regression, and wavelet architectures for trend monitoring, detection, and analysis of meaningful variations in physiological signals. The implemented trend detection methods have been applied to the physiological signals pertinent in conjunction with the tasks of monitoring wounded soldiers at the battlefield and pilots in high-acceleration environment. Performance, robustness, and speed of operation of these methods have been then investigated, analyzed, and compared in view of real-time monitoring requirements characteristic of the military applications. In conclusion, from the study performed in this work we can infer the following observations:

TABLE II
COMPARISON RESULTS FOR THE FIVE TREND DETECTION APPROACHES WHEN USED TO IDENTIFY TRENDS IN THE HEARTBEAT RATE SIGNAL SHOWN IN FIG. 14

APPROACH APLLIED TO HEARTBEAT RATE SIGNAL (OVERLAPPING WINDOWS)	**TREND/SHAPE** (BY VISUAL INSPECTION) **Seg1: decrease, concave downward Seg2: increase, concave upward Seg3: variable, almost unchanged**	**TREND DETECT**	**SHAPE DETECT**	**COMPUTATION TIME** (IN MATLAB 6.0 ENVIRONMENT)
Fuzzy Noise-rejection	Seg1: decrease, concave downward	√	√	4 seconds
	Seg2: increase, concave upward	√	√	
	Seg3: variable almost unchanged	√	√	
Fuzzy Course	Seg1: decrease, concave upward	√	×	2.6 seconds
	Seg2: increase, concave upward	√	√	
	Seg3: linear increase	×	×	
Trigg's Statistical	Seg1: decrease	√	×	3.7 seconds
	Seg2: increase	√	×	
	Seg3: decrease	×	×	
Temporal Reasoning	Seg1: decrease, concave downward	√	√	5.5 seconds
	Seg2: increase, concave upward	√	√	
	Seg3: increase downward	×	×	
Wavelet Decomposition	Seg1: decrease, concave downward	√	√	1.3 seconds
	Seg2: increase, linear	√	×	
	Seg3: decrease, linear	×	×	

TABLE III
COMPARISON RESULTS FOR THE FIVE TREND DETECTION APPROACHES WHEN APPLIED TO THE ANALYSIS OF TRENDS IN THE SYNTHETIC OPACITY SIGNAL SHOWN IN FIG. 15

APPROACH APPLIED TO SYNTHETIC OPACITY SIGNAL (NONOVELAPPING WINDOWS)	**TREND/SHAPE** (BY VISUAL INSPECTION) **Seg1: decrease, concave downward Seg2: increase, concave downward**	**TREND DETECT**	**SHAPE DETECT**	**COMPUTATION TIME** (IN MATLAB 6 ENVIRONMENT)
Fuzzy Noise-rejection	Seg1: decrease, concave downward	√	√	2.5 seconds
	Seg2: increase, concave downward	√	√	
Fuzzy Course	Seg1: decrease, concave downward	√	√	1.6 seconds
	Seg2: increase, concave downward	√	√	
Trigg's Statistical	Seg1: decrease	√	×	2.5 seconds
	Seg2: increase	√	×	
Temporal Reasoning	Seg1: decrease, concave downward	√	√	4.1 seconds
	Seg2: increase, concave downward	√	√	
Wavelet Decomposition	Seg1: decrease, linear	√	×	1.3 second
	Seg2: increase, linear	√	×	

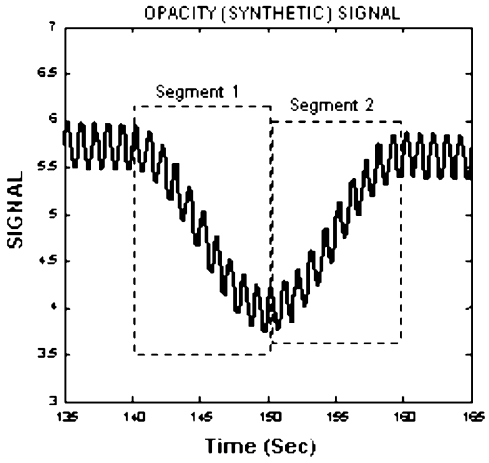

Fig. 15. A 30-s-long portion of a synthetic opacity signal considered in the third comparison.

For blood pressure, or heartbeat signals that embody several higher-frequency components similar to those used in the above comparisons, temporal reasoning and fuzzy logic approaches are the most suitable due to their very low susceptibility to signal fluctuations and noise. In specific terms, temporal reasoning approach uses the first and second derivatives of a fifth-order polynomial fit to the actual signal to detect the shape of a trend and hence provides high accuracy in the presence of high-frequency oscillations and noisy components. Moreover, fuzzy noise-rejection and course approaches are both suitable herein for trend detection in real physiological signals thanks to their ability to identify underlying trends during high fluctuations in a signal and also in the presence of noisy information.

For signals such as opacity (synthetic ear opacity in Fig. 15) in the presence of higher oscillations, fuzzy and temporal approaches again showed the highest accuracy among all tested approaches in identifying the trend and its shape.

If the speed of computation during signal monitoring is an important factor, it might render approaches such as fuzzy course and regression a liability. Therefore, these techniques should be used for trend detection when speed of computation is not critical.

The Trigg's approach, which is suitable for short-term monitoring is recommended if speed of computation is a factor. In our comparison, this approach proved to be very consistent in identifying trends in various experimental and synthetic signals. Hence, unless shapes of a trend (concave down, etc.) are of critical importance, one should consider using the statistical detection approach for short-duration monitoring where speed of computation and software latency play a role in successful physiological signal assessment.

The wavelet decomposition approach is recommended for extremely noisy signals where only the underlying trend needs to be identified. In other words, wavelet decomposition allows for extraction of the slowest part of a signal and hence the identification of the trend would be a less challenging task. However, from the above analysis we can see that the accuracy results where mixed, thereby indicating that the approach sometimes detect trends but not shapes, and in some other times even fail to detect the underlying trend.

In our current continuation work, trends in a physiological signal are generically treated as output observations resulting from variations and patterns in associated input variables that directly affect this physiological signal. Thereby, we develop a so-called trend modeling methodology in which a trend of a physiological signal is treated as a dependent variable in an input(s)–output(s) relationship. Independent variables in this relationship are other physiological signals whose "actual" real-time variations, as well as meaningful trends give rise to corresponding trends in the dependant physiological signal. Having established such an input-output relationship, a trend model of a physiological phenomenon would incorporate independent variables and their trends as inputs. The outputs will be physical values, as well as possible trends in a physiological signal of interest. In this manner, the trend model of a system would yield a generic-form dynamic model that predicts the behavior of output variables, given values of its inputs in real-time or pseudo real-time.

REFERENCES

[1] C. Tsien, "Trend Finder: Automated detection of alarmable trends," Ph.D. dissertation, Massachusetts Inst. Technol., Cambridge, MA, 2000.

[2] F. Steimann, "Diagnostic monitoring of clinical time series," Ph.D. dissertation, Technische Universitat Wien, Wien, Austria, 1996.

[3] R. Allen, "Time series methods in the monitoring of intracranial pressure I: Problems, suggestion for a monitoring scheme and review of appropriate techniques," *J. Biomed. Eng.*, vol. 5, pp. 5–17, 1983.

[4] J. A. Blom, J. F. Ruyter, N. Saranummi, and J. W. Beneken, "Detection of trends in monitored variables," in *Computer and Controls in Clinical Medicine*, E. R. Carson and D. G. Cramp, Eds. New York: Plenum, 1985, pp. 153–174.

[5] R. E. Challis and R. I. Kitney, "Biomedical signal processing: Part I: Time domain methods," *Med. Biol. Eng. Comput.*, vol. 28, pp. 509–524, 1990.

[6] I. J. Haimowitz and I. S. Kohane, "Automated trend detection with alternative temporal hypotheses," in *Proc. 13th Int. Joint Conf. Artificial Intelligence IJCAI-93*, Chamberey, France, 1993, pp. 146–151.

[7] V. Hiranmayee and V. Venkat, "A wavelet theory-based adaptive trend analysis system for process monitoring and diagnosis," in *Proc. American Control Conf.*, 1997, pp. 309–313.

[8] F. Flehming, R. V. Watzdorf, and W. Maquardt, "Identification of trends in process measurements using a wavelet transform," *Comput. Chem. Eng.*, vol. 22, pp. S491–S496, 1998.

[9] R. R. Kennedy, "A modified Trigg's tracking variable as an advisory alarm during anaesthesia," *Int. J. Clin. Monitor. Computing*, vol. 12, pp. 197–204, 1995.

[10] E. Hope, C. D. Lewis, I. R. Perry, and A. Gamble, "Computed trend analysis in automated patient monitoring systems," *Br. J. Anaesth.*, vol. 45, pp. 440–448, 1973.

[11] B. Konstantinov and T. Yoshida, "Real-time qualitative analysis of temporal shapes of (bio) process variables," *AIChE J.*, vol. 38, no. 11, pp. 1703–1715, 1992.

[12] J. C. Bezdek, *Pattern Recognition with Fuzzy Objective Function Algorithms*. New York: Plenum, 1981.

[13] J. H. Ward, "Hierarchical grouping to optimize an objective function," *J. Am. Statist. Assoc.*, no. 58, pp. 236–244, 1963.

[14] W. W. Melek, M. R. Emami, and A. A. Goldenberg, "An improved robust fuzzy clustering algorithm," in *Proc. IEEE Int. Fuzzy Systems Conf.*, vol. 3, Seoul, Korea, 1999, pp. 1261–1265.

[15] R. Krishnapuram and O. Nasouri, "An improved possibilistic c-means algorithm with finite rejection and robust scale estimation," in *New Frontiers in Fuzzy Logic and Soft Computing Biennial Conf. NAFIPS*, 1996, pp. 395–399.

William W. Melek (M'03) received the B.A.Sc. degree in electrical engineering from Zagazig University, Cairo, Egypt, in 1994, and the M.A.Sc. and Ph.D. degrees in mechanical engineering from the University of Toronto, Toronto, ON, Canada, in 1998 and 2002, respectively.

From 1994 to 1996, he was with by Siemens Ltd., Cairo, Egypt, where he worked mainly on control and analysis of drive mechanisms. During this period, he also served as a Software Consultant with the Egyptian Government Institute of Technology, Cairo, Egypt. From 2000 to 2002, he served as the Research Administrator of the Robotics and Automation Laboratory at the University of Toronto. During such period, he also served as a Senior Consultant for Engineering Services Inc. Toronto, ON, Canada, where his work mainly focuses on developing advanced modeling techniques for defence applications. Between 2002 and 2004, he held the position of AI Division Manager with Alpha Global IT Inc., Toronto, ON, Canada. He is currently an Assistant Professor with the Department of Mechanical Engineering, University of Waterloo, Waterloo, ON, Canada. His current research interests include mechatronics applications, robotics, industrial automation and the application of fuzzy-logic, neural networks, and genetic algorithms for modeling and control of dynamic systems.

Dr. Melek is a Member of American Society of Mechanical Engineers.

Ziren Lu received the B.Sc. degree in mechanical engineering from East China University of Science & Technology, Shanghai, China, in 1982, the M.Sc. degree in electronic engineering from the Shanghai Jiao Tong University, Shanghai, China, in 1986, and the Ph.D. degree from the University of Toronto, Toronto, ON, Canada.

Currently, he is a Senior Research Engineer and System Designer in Security and Defense Division, Engineering Services Inc. (ESI), Toronto, ON, Canada. His research interests include system modeling, control and knowledge-based systems.

Alex Kapps received the B.Sc. degree in aeronautical engineering from the Technion-Israel Institute of Technology, Haifa, Israel, in 1985, the M.Sc. degree in mechanical engineering from Tel-Aviv University, Tel-Aviv, Israel, in 1990 and the Ph.D. degree from the University of Toronto, Toronto, ON, Canada, in 1993.

From 1985 to 1988, he worked as a Technical Officer in the Headquarters of the Israeli Air Force. From 1988 to 1990, he worked at MAGASH Systems Ltd. (presently Image Information Technologies Ltd.), Tel-Aviv, and also served as a consultant to the Israeli Institute of Innovations. In 1993, he joined Engineering Services Inc. where he has since been working as a Senior Systems Designer, Project Leader, and Division Manager. His current research interests and work at ESI are in the area of decision support systems, adaptive feedback control, data acquisition and signal processing, dielectric elastomer actuators and sensors and MEMS gas sensors.

Dr. Kapps is a member of the Professional Engineers of Ontario.

William D. Fraser, photograph and biography not available at the time of publication.